




Isolation of native EVs from primary biofluids—Free-flow electrophoresis as a novel approach to purify ascites-derived EVs

Christian Preußner^{1,2}  | Kathrin Stelter¹ | Tobias Tertel³ | Manuel Linder¹ |
 Frederik Helmprobst⁴ | Witold Szymanski⁵ | Johannes Graumann⁵  | Bernd Giebel³ |
 Silke Reinartz⁶ | Rolf Müller⁶ | Gerhard Weber⁷ | Elke Pogge von Strandmann^{1,2} 

¹Institute for Tumor Immunology, Center for Tumor Biology and Immunology, Philipps University Marburg, Marburg, Germany

²Core Facility Extracellular Vesicles, Center for Tumor Biology and Immunology, Philipps University of Marburg, Marburg, Germany

³Institute for Transfusion Medicine, University Hospital Essen, University of Duisburg-Essen, Essen, Germany

⁴Core Facility for Mouse Pathology and Electron Microscopy, Institute of Neuropathology, Philipps University Marburg, Marburg, Germany

⁵Institute of Translational Proteomics, Philipps University of Marburg, Marburg, Germany

⁶Translational Oncology Group, Center for Tumor Biology and Immunology, Philipps University Marburg, Marburg, Germany

⁷FFE Service GmbH, Feldkirchen, Germany

Correspondence

Institute for Tumor Immunology, Center for Tumor Biology and Immunology, Philipps University Marburg, Marburg, Germany.
 Email: poggevon@staff.uni-marburg.de

Funding information

Deutsche Forschungsgemeinschaft, Grant/Award Numbers: GRK2573, KFO325 to EPvS

Abstract

Although extracellular vesicles (EVs) have been extensively characterized, efficient purification methods, especially from primary biofluids, remain challenging. Here we introduce free-flow electrophoresis (FFE) as a novel approach for purifying EVs from primary biofluids, in particular from the peritoneal fluid (ascites) of ovarian cancer patients. FFE represents a versatile, fast, matrix-free approach for separating different analytes with inherent differences in charge density and/or isoelectric point (pI). Using a series of buffered media with different pH values allowed us to collect 96 fractions of ascites samples. To characterize the composition of the individual fractions, we used state-of-the-art methods such as nanoflow and imaging flow cytometry (nFCM and iFCM) in addition to classical approaches. Of note, tetraspanin-positive events measured using nFCM were enriched in a small number of distinct fractions. This observation was corroborated by Western blot analysis and electron microscopy, demonstrating only minor contamination with soluble proteins and lipid particles. In addition, these gently purified EVs remain functional. Thus, FFE represents a new, efficient and fast method for separating native and highly purified EVs from complicated primary samples.

KEYWORDS

ascites, extracellular vesicles, free-flow electrophoresis, microvesicles

1 | INTRODUCTION

Extracellular vesicles (EVs) are biological nanoparticles that are secreted by virtually every cell into the extracellular environment and can be found in all tissues and biofluids. These vesicles, especially the endosomal-derived exosomes and plasma-membrane origin ectosomes or microvesicles, play important roles in physiological and pathophysiological intercellular communication and act as transmitters of various cargoes such as nucleic acids, proteins, lipids, and metabolites (for review see van Niel et al., 2018)

Being assembled in cell-type-specific manners, EVs are considered as a promising class of novel biomarkers for various diseases including tumours and proinflammatory diseases such as COVID-19 (Dörsam et al., 2018; Tertel et al., 2022).

This is an open access article under the terms of the [Creative Commons Attribution-NonCommercial-NoDerivs License](https://creativecommons.org/licenses/by-nc-nd/4.0/), which permits use and distribution in any medium, provided the original work is properly cited, the use is non-commercial and no modifications or adaptations are made.

© 2022 The Authors. *Journal of Extracellular Biology* published by Wiley Periodicals, LLC on behalf of the International Society for Extracellular Vesicles.

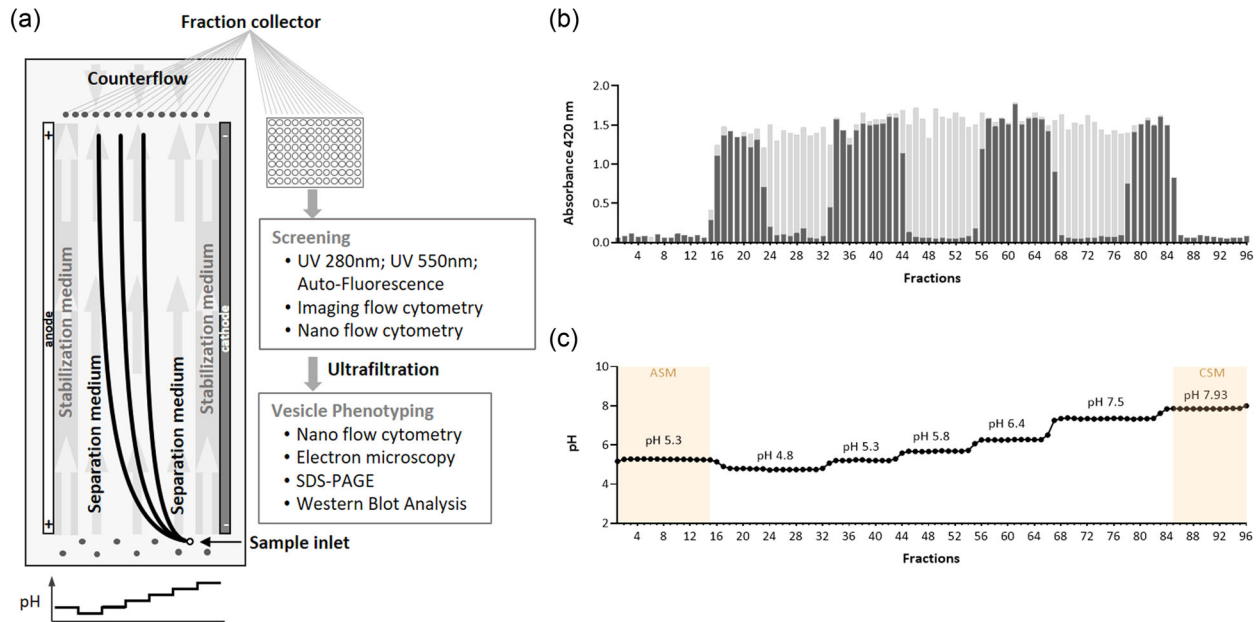


FIGURE 1 Free flow electrophoresis as an isolation method for EVs from ascites. (a) Schematic overview and workflow of the FFE device: Analytes loaded into the sample inlet are transported by a longitudinal flow and separated in a vertical electric field. The migration speed of the specific analytes within the electric field depends on their isoelectric points and pH values of the separation buffers in the separation area. To avoid the analytes contacting neither the cathode nor the anode, stabilizing buffers with higher pH values sheath the electrodes. After separation, the different analyses are adjusted to a neutral pH by a counterflow using a corresponding buffer. Through tubes connected with the separation chamber, the analytes are collected in a 96-well plate and the cavities were initially analyzed by UV spectroscopy, imaging, and nanoflow cytometry. Subsequently, selected fractions were concentrated by ultrafiltration, and the resulting samples were further characterized according to MISEV criteria. (b) Prior to sample loading, the performance of the separation cell and the selected protocol, as well as, the composition of the individual media were tested to ensure their performance. Using a dye, tubing, laminar flow, and pump parameters were tested. Shown are two stripe tests in which four individual stripes are visible (dark grey) and a uniform and continuous distribution of the samples (light grey bars). (c) Quality control of the media. Buffers according to the selected 5-step protocol (pH 4.8 - pH 7.5) were injected into the chamber without applying any current and collected in a 96-well plate. The pH values of the individual cavities were determined and plotted. In addition, stabilization buffers (ASM; CSM) can also be detected

Although EVs have been characterized to some extent and a wide variety of purification techniques have been described, the separation of EVs from other extracellular particles (EPs) remains challenging, especially for primary bioliquids such as blood plasma, blood serum, or ascites (Clayton et al., 2019). In such fluids, the diversity and intricate association of biomolecules complicate the preparation of high-purity EVs even when using stringent techniques such as density gradient centrifugation, and may require different methods in sequence (Karimi et al., 2018; Tulkens et al., 2020). Often, a compromise between quality and quantity must be struck, limiting initial characterization of certain EV types. Moreover, the choice of the purification method may affect EV integrity and composition, especially if particles are subjected to excessive force, for example, during ultracentrifugation (Linares et al., 2015).

The individual EV subtypes are even more challenging to separate from each other as they may differ only slightly in their physical properties such as size and density (van der Pol et al. 2014; Witwer & Théry, 2019). However, by implementing new methods such as asymmetrical flow field-flow fractionation (Zhang & Lyden, 2019), an increasing number of efforts were made to separate the different subtypes based on, albeit minor, variations in their properties.

One of these new approaches is represented by free-flow electrophoresis (FFE), a well-established matrix-free, liquid-based, highly versatile technology for separating analytes according to their net charge. A variety of approaches can be used in FFE, like interval zone electrophoresis with different pH steps. Here, buffers with different pH values are introduced into a separation chamber via vertically arranged inlets at the bottom of the chamber, creating a continuous laminar flow of distinctly defined pH zones along the longitudinal axis. After sample injection through one of the buffer inlets, the sample is transported by the laminar flow of the aqueous medium. Subsequently, a high voltage perpendicular to the laminar flow direction is applied by two electrodes (anode and cathode) flanking the separation chamber, which results in the deflection of the respective analytes in the laminar film according to their mobility and their isoelectric point, depending on the pH values of the buffers introduced. Once the samples have passed through the separating chamber, samples are adjusted to a neutral pH using an appropriate counterflow and finally collected through a 96-outlet tubing into a 96-well plate. Because of its versatile protocols, FFE can be used as a preparative method in combination with its semi-analytical features (Figure 1a) (Krivánková & Bocek, 1998; Staubach et al., 2022; Weber et al., 2004).

Like the plasma membrane, EVs exhibit a surface charge (zeta potential) that generally appears negative due to the lipids and the embedded glycosylated proteins (Akagi & Ichiki, 2008), thereby qualifying EVs perfectly for separation by FFE. Since the zeta potential depends on many factors such as membrane surface group composition, ionization, as well as adsorption of electrolytes present in the solution, the FFE provides, in addition, the potential to separate subpopulations of differently charged vesicles.

While FFE purification of EVs was initially described for defined cell culture supernatants, in particular from mesenchymal stromal cell (MSC) conditioned media (Staubach et al., 2022), these protocols were based on low protein input and a resulting low conductivity.

Here, we present a protocol that allows the isolation of EVs from peritoneal fluid of ovarian cancer patients (ascites), a highly complex biofluid with clinical prognosis value, using FFE. With the FFE approach presented here, and in line with the MISV guidelines (Théry et al., 2018), we demonstrated that by using a combination of classical methods as well as second-generation approaches such as nano- and imaging-flow cytometry, we are able to enrich bona fide ascites-derived EVs using FFE, further establishing this method as a versatile and robust EV separation technology to be implemented in future studies.

2 | MATERIALS AND METHODS

2.1 | Ascites

Ascites were collected from untreated high-grade serous ovarian carcinoma patients undergoing first-line surgery at the University Hospital Marburg (Marburg, Germany). Informed consent was obtained from all patients according to the protocols approved by the institutional ethics committee (reference number 205/10). Cells were removed by centrifugation at 300×g for 10 min at 4°C, followed by a second centrifugation step at 2500×g for 10 min at 4°C. Cell-free ascites supernatants were cryopreserved at −80°C for later use.

2.2 | FFE separation

FFE experiments were performed on an FFE NextGen system (FFE Service GmbH, Feldkirchen, Germany), equipped with nine inlets for loading separation buffers and three inlets for loading counterflow buffers at the terminus of the separation chamber. All separations were performed using a 500 mm × 100 mm separation chamber with a gap width of 0.2 mm between a transparent front plate and a cooled metal back plate. The separation media were introduced via nine inlets by a peristaltic pump, passed through the separation chamber, and fractions were collected via an outlet set of 96 tubes with an inner diameter of 0.35 mm into the collection plate. 96-transwell plates were used, with a collection time ranging from 5 to 8 min. Four millilitres of ascites samples from three individual patients which were pre-cleared by centrifugation at 2,000×g for 3 min, and subjected to FFE. A continuous mode was used to process large sample volumes and collected into 96 fractions of deep-well plates (DWP) (2 ml capacity/well). The ascites samples were diluted by a factor of four with one of the separation media, and sample application was performed using an independent controlled dual-port peristaltic pump. The sample injection rate was 6 ml/h and the turn-around time for each sample through the system was less than 7 min followed by the collection (5–8 min). Application of 1,000–1,250 V established the electric field for separation and the heat generated was dissipated through a cooled metal back plate, stabilizing the temperature in a 5°C–7°C range. The entire system was controlled by a microprocessor control unit displaying the operation parameters.

2.3 | Spectroscopic analyses and pH measurements

Spectroscopic analyses of the collected fraction were done in 96-well plates using a microplate reader (Tecan M200, Tecan, Männedorf, Switzerland) equipped with UV-vis and fluorescence detectors. The protein content was measured by absorbance at 280 nm excitation and additionally, autofluorescence was determined at 350 nm (10 nm bandwidth, photomultiplier gain 80). The turbidity of each sample was measured at 515 nm. Absorbance profiles were plotted in programs.

pH was measured by an automated Tecan MSP9259 microplate robotic system, (Tecan) equipped with a WTW inoLab pH730 pH-meter (inoLab, Weilheim, Germany).

2.4 | Imaging flow cytometry

Ten microlitres of an antibody mix containing 0.5 μl PE-conjugated anti-human CD9 (EXBIO, Vestec, Czech Republic), 0.5 μl APC-conjugated anti-human CD63 (EXBIO, Vestec, Czech Republic), and 0.5 μl FITC-conjugated anti-human CD81 (Beckman Coulter, Krefeld, Germany) were added to 90 μl of each fraction. Unstained samples or dilutions of the antibody mix in respective buffers were used as controls as recommended by the MIFlowCyt-EV framework (Welsh et al., 2020). After incubation for 1 h at

room temperature, samples were analyzed using the built-in autosampler from U-bottom 96-well plates (Corning, Kaiserslautern, Germany) with an ImageStreamX Mark II instrument (Amnis/Luminex, Seattle, WA, USA). All data were acquired with 5 min acquisition time at 60x magnification at a low flow rate ($0.3795 \pm 0.0003 \mu\text{l}/\text{min}$) and with removed beads option deactivated as described previously. Data analysis was performed using IDEAS software version 6.2 as previously described (Tertel, Bremer, et al., 2020; Tertel, Görgens, et al., 2020). All fluorescent events were plotted against the side scatter. Images were analyzed for coincidences by using the spot-counting feature. Events with multiple spots were excluded from further analysis. All remaining events with low SSC (<500) and a fluorescent intensity higher than 300 were included in the calculation of concentrations. Further details are provided in Supplementary Table S1.

2.5 | SDS-PAGE and Western blotting

Five microlitres of each indicated FFE fraction was incubated with 4x SDS sample buffer and run on a 10% SDS protein gel, followed by Coomassie-staining. For western blot analysis, 5×10^8 EVs in 1x PBS were lysed in 10x RIPA buffer followed by the addition of 4x SDS sample buffer prior to loading on a 10% SDS protein gel. Proteins were transferred to a nitrocellulose membrane (GE Healthcare, Freiburg, Germany), and membranes were blocked with 5% (w/v) milk powder (Carl Roth, Karlsruhe, Germany) in Tris-phosphate-buffered saline supplemented with 0.05% Tween (TBS-T) for 1 h. Subsequently, membranes were probed with indicated antibodies (see Supplementary Table S1). Detection was performed with horseradish peroxidase-conjugated secondary antibodies (DAKO, Hamburg, Germany) using Amersham ECL Plus (GE Healthcare, Freiburg, Germany).

2.6 | Nanoflow cytometry (nFCM)

For nFCM, a Flow NanoAnalyzer (NanoFCM Co., Ltd, Nottingham, UK) equipped with a 488 nm laser, was calibrated using 200 nm polystyrene beads (NanoFCM Co.) with a defined concentration of 2.08×10^8 particles/ml, which were also used as a reference for particle concentration. In addition, monodisperse silica beads (NanoFCM Co., Ltd, Nottingham, UK) of four different diameters (68 nm; 91 nm; 113 nm; 155 nm) served as size reference standards. Freshly filtered ($0.22 \mu\text{m}$) 1x PBS was analyzed to define the background signal, which was subtracted from all other measurements. Each distribution histogram or dot plot was derived from data collected for one minute with a sample pressure of 1.0 kPa. The EV samples were diluted with filtered ($0.1 \mu\text{m}$) 1x PBS, resulting in a particle count in the optimal range of 2,500–12,000 events. Particle concentration and size distribution were calculated using NanoFCM software (NF Profession V1.08).

For immunofluorescent staining, $12.5 \mu\text{M}$ of corresponding antibodies in $50 \mu\text{l}$ 1x was used (for antibodies see Supplementary Table S1). After removing antibody aggregates by centrifugation at $12,000 \times g$ for 10 min, the supernatant was added to 2×10^8 particles, followed by incubation for 2 h at 30°C under constant shaking and washing with 1 ml 1x PBS by ultracentrifugation at $110,000 \times g$ for 45 min at 4°C (Beckman Coulter MAX-XP centrifuge, TLA-145 rotor; Beckman Coulter, Krefeld, Germany). The pellet was resuspended in $50 \mu\text{l}$ 1x PBS for nFCM analysis. Each sample was diluted at 1:10 in 1x PBS and detection was set to 3,000 events.

2.7 | Electron microscopy

EVs were prepared for electron microscopy as described previously (Théry et al., 2006) with few modifications. Briefly, EVs were fixed with an equal amount of 4% PFA. Fixed EVs ($5\text{--}7 \mu\text{l}$ of the solution) were placed on Formvar/carbon-coated 200 mesh copper grid (Ted Pella Inc., Redding, USA) and incubated, washed, and fixed with 1% glutaraldehyde, as described in the cited protocol. After eight additional washing steps with sterile filtered water, EVs were incubated with 1% uranyl acetate for 5 min. The grid was dipped onto a drop of 2% methylcellulose supplemented with 4% uranyl acetate (ratio 9:1) on ice. Excess fluid was removed with filter paper and the samples were air-dried for up to 10 min. Images were taken with a Zeiss EM 900 at 80 kV.

3 | RESULTS

3.1 | Optimizing FFE for EV isolation

The current FFE protocol was established for the separation of defined culture supernatants supplemented with human platelet lysate (Staubach et al., 2022) and cannot be applied for the enrichment of EVs from more complex biofluids. We, therefore, developed a new protocol and used the bases histidine (pKa 6) and BISTRIS (pKa 6.5) together with propionic acid (pKa = 5) in the respective separation buffer, providing a significant improvement compared to previous combinations used in the FFE

TABLE 1 FFE media for a five-step pH gradient

Inlets	E1	E2	E3	E4	E5	E6	E7	E8	E9
Media	ASM								CSM
pH	5.3	4.8	4.8	5.3	5.8	6.4	7.5	7.93	
Conductivity [μ S]	7,850	2,000	500	500	500	500	500	5,930	

ASM, anodic stabilization medium; CSM, cationic stabilization medium.

protocols (e.g., TRIS, pKa 8.4 as a base and acetic acid as acid). As the pKa values of the bases and acids are within the desired pH range (4.8–7.3) of all separation media used, a significantly improved buffer capacity of all separation media is achieved. This allows the processing of higher protein quantities and simultaneously maintains constant pH values in the respective separation media to avoid uncontrolled precipitation of protein. In addition, we used propionic acid instead of acetic acid, which is commonly used in FFE. This allows the use of separation media with lower conductivity values and simultaneously the use of higher voltages together resulting in improved separation performance during the purification process (Table 1, patent pending).

To adapt this technique for the separation and preparation of EVs from primary biofluids (here human ascites), and to subsequently characterize the EVs in detail, our general strategy is shown in Figure 1a. First, the pH and conductivity of the distinct buffers used were adjusted according to the selected protocol (Table 1). Before loading the FFE separation chamber, the appropriate assembly of the FFE device and the performance of the electrophoresis chamber were verified. Initially, the performance of the individual inlets (E1–E9) contributing to the laminar flow was examined using a so-called stripe test (Figure 1b), in which seven inlets were filled alternating with water or SPANDS-coloured water (sulfanilic acid azochromotrop), resulting in four red stripes. Furthermore, all seven inlets were used to fill the chamber with SPANDS-coloured water to subsequently monitor a uniform laminar flow across the effective separation space (fractions F16–F85) (Figure 1b). After these initial tests, the actual separation buffers were introduced. After flushing the separation chamber for 10 min with a continuous flow of 250 ml/h, the correct position of the media and the resulting pre-formed five-step pH gradient (4.8; 5.3; 5.8; 6.4; 7.5) flanked by the anode- and cathode-stabilization buffers (pH 5.3 and pH 7.93, respectively), were controlled (Figure 1c). Once the final process parameters had been defined using these tests, a constant high voltage of 1200 V was applied at a flow rate of 80 ml/h, and a pI mix was introduced thus assaying the running parameters and stability of the gradient during electrophoresis conditions. After 6 min, 200 μ l of buffer was collected and the pherogram of the pI-marker as well as the gradient was determined by pH measurement (Figure 1c + Supplementary Figure S1).

3.2 | The optimized FFE protocol allows a fast and highly reproducible separation of the ascites secretome

To utilize the FFE for the separation of EVs from other ascites components, three individual patient samples (each 4 ml) were pre-cleared by centrifugation at 2,000 \times g for 3 min. In the following, 2 ml of pre-cleared ascites were mixed 1:4 with buffer pH 7.5, and subsequently, samples were sequentially injected into the separation chamber via the dosing tube in inlet E8. Initially, 96 fractions (200 μ l each) were collected for 6 min into multi-transwell plates (MTP). In continuous separation mode, 96 fractions were collected during 120 min into 4 ml DWP. Both, anode (F1–F15), as well as cathode (F86–F96) stabilization buffers, were included in the 96 fractions.

The protein content of the respective fractions was spectroscopically determined by analyzing the absorbance at UV280 nm and UV550 nm as well as measuring auto-fluorescence (emission at 350 nm) (Figure 2a). The protein appeared distributed across the entire separation range with notable accumulations in fractions F18, F24, and F36. The profile was reproducible for all three biological replicates (Supplementary Figure S2).

In addition, initial experiments showed that we can also apply the FFE protocol to other biofluids, such as blood plasma and serum (Supplementary Figure S3).

Due to their molecular composition and the resulting negative zeta potential, EVs are expected to predominantly accumulate in the anterior fractions with lower pH. Consequently, we focused our subsequent analyses on fractions F1–F48. As a first readout, these fractions of all three independent runs were separated on SDS-PAGE (Figure 2b). Coomassie staining of the gels confirmed the results of the spectral analyses and furthermore demonstrated variably protein complexities in the different samples.

3.3 | FFE facilitates the enrichment of bona fide EVs from human ascites

To characterize the individual fractions in more detail and especially for their putative EV content, the particle concentration of the first 48 fractions was determined by nFCM. We chose nFCM, because it (1) allows a higher sample throughput on the

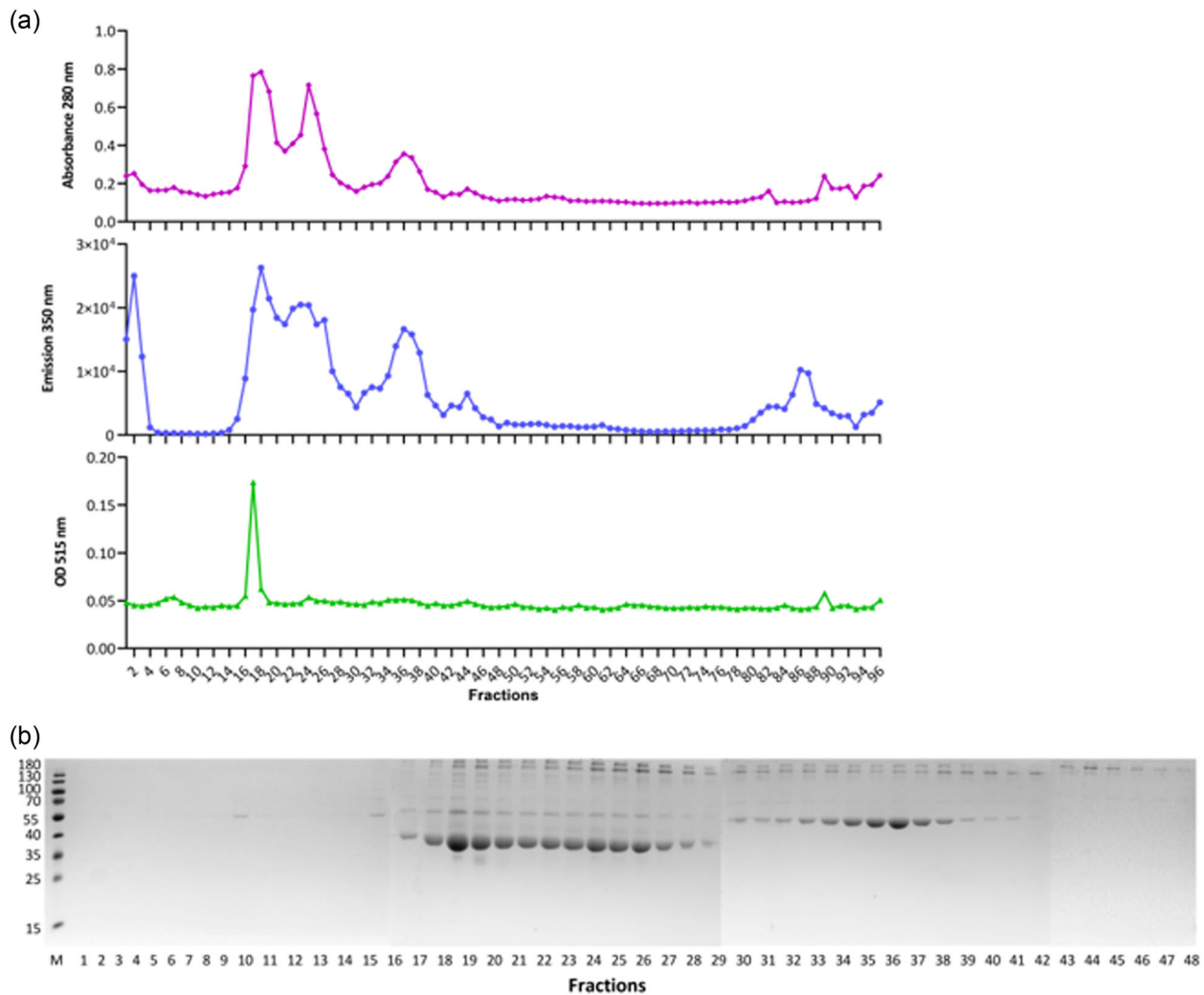


FIGURE 2 FFE separates efficiently the ascites secretome. (a) Representative programs of applied and FFE-processed ascites samples. The collected 96 fractions were analyzed by UV-spectroscopy detecting absorbance at 280 nm and autofluorescence (extinction 280 nm, emission 350 nm, panel b). (b) Protein distribution of FFE-separated ascites samples. The first 48 fractions were analyzed by SDS-PAGE and Coomassie staining. Markers in kDa

single vesicle levels; (2) minimizes measurement failures due to prior calibration; and (3) allows a more specific phenotypic characterization of possible EVs in subsequent downstream analyses.

An elevated particle concentration ranging from 1 to 1.5×10^{10} particles/ml was detected in fractions F16–F18 for all three replicates (Figure 3a; Supplementary Figure S4A+B), in which less protein could also be detected spectroscopically (Figure 2a). To assess the presence of established EV markers, we probed the fractions for EV-associated tetraspanins CD9, CD63, and CD81 by iFCM (Figure 3b; Supplementary Figure 4A+B). In each patient sample, all tested tetraspanins could be detected, with some variation in intensities between samples, as one could expect for primary biomaterials. Furthermore, CD9+, CD81+, and CD63+ events are focused on a few distinct fractions (F15–F20). Strikingly, the fractions with enriched particle concentrations are also those with greatest tetraspanin positivity, suggesting that the particles detected are enriched in EVs.

These results were verified in the main as well as flanking fractions (F15–F20) by Western blot (Figure 4). In addition, two later fractions (F25 + F32) were included as controls, exhibiting only low particle concentration and low tetraspanin intensities. In the three main fractions (F17–19), the two intravesicular markers ALIX and flotillin-1 could also be detected. Since primary biofluids such as plasma and ascites may also contain many non-EV EPs, the presence of lipid particles such as HDL, LDL, and VLDL was also assessed by checking the presence of apolipoproteins. Although ApoA (HDL marker) could be detected in the ascites input, no signal was observed in the examined FFE fractions. In the case of ApoE (chylomicron/VLDL marker), however, a clear signal was detected in fraction F18. Note that ApoE was also reported to be associated with EVs (van Niel et al., 2015).

Finally, to further increase the EV concentration and minimize any free protein contaminants, we pooled the three fractions with the highest particle concentrations and tetraspanin-positive events (F16-18) and the sample volume (1.5 ml) was reduced to

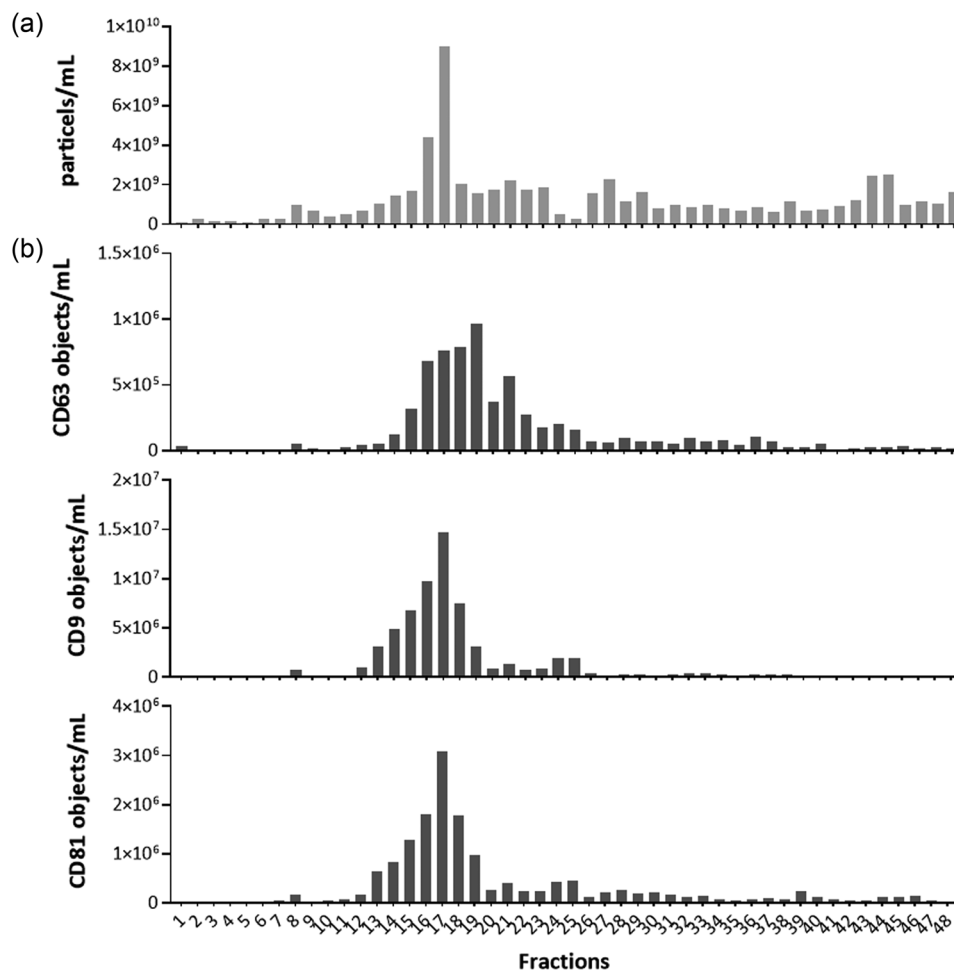


FIGURE 3 Tetraspanin-positive particles are concentrated in discrete fractions. (a) Particle concentration of the first 48 fractions was determined by nanoflow cytometry (nFCM). Concentrations show a relatively high particle concentration in fractions 16–18. Shown are measured particles per mL sample. (b) FFE fractions were analyzed by imaging flow cytometry (IFCM) concerning their phenotypic properties of CD63, CD9, and CD81. Fractions 15–19 show detectable signals for all three tested markers

approximately $50 \mu\text{l}$ by ultrafiltration (300 kDa cut-off). This pool we consider as the final EV sample, which in sum originated from a pre-cleared ascites input and was subjected solely to FFE and a subsequent ultrafiltration step.

To further characterize these EVs, we subjected them to electron microscopy (Figure 5a). The negative-contrasted images show EV-typical particles and, no typical indications of protein contamination. Furthermore, we did not observe lipid particles.

Finally, we performed single-EV phenotyping of concentrated EVs using nFCM. The three tetraspanin markers CD9, CD63, and CD81 were detected with different efficiencies. With 48.6%, CD9 was detected on the largest percentage of all detected particles, followed by CD81 (24.4%) and CD63 (13.6%). In addition, 12% of particles, were double-positive for CD9 and CD63. Furthermore, the epithelial cell adhesion molecule EpCAM was detected on 13.2% of particles (Figure 5b,c) indicating that these EVs were derived from tumour cells. The diameter of positive particles was also measured, with tetraspanin-positive particles ranging from 77 to 89 nm, whereas EpCAM-positive events exhibited an average diameter of approximately 95 nm (Figure 5d).

To test whether the FFE-separated ascites EVs were functionally active, we used a fibroblast activation assay which was adapted from Dörsam et al. (2018), resulting in induction of several inflammatory fibroblast markers, including CXCL1, CXCL8, and IL-6 (Supplementary Figure S5). In addition, expression of αSMA and COL1A1 was decreased, indicating fibroblast activation towards an inflammatory phenotype.

4 | DISCUSSION

Since their discovery, and particularly within the last decade, interest in EVs and their specific purification has grown continuously. Due to the large number of diverse EPs released by cells into the extracellular environment, stringent purification remains

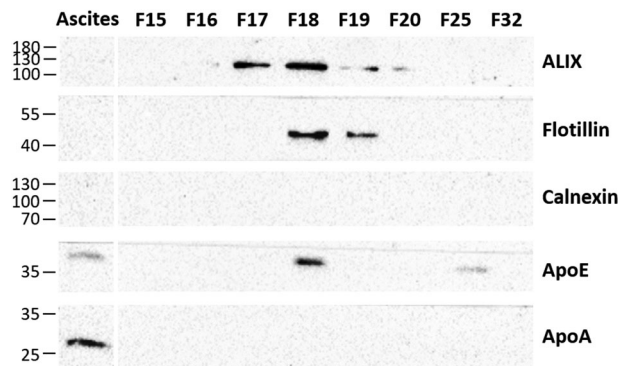


FIGURE 4 Characterization of ascites-derived FFE-isolated EVs. Western blot analyses for intravesicular markers. 5×10^8 particles were lysed in RIPA 10X buffer and resolved on SDS-PAGE (10% gels). Intravesicular markers Alix (98 kDa), Flotillin (47 kDa), and calnexin (90 kDa) as a negative markers as well as the two apolipoproteins ApoE (34 kDa) and ApoA (29 kDa) were detected. Markers in kDa

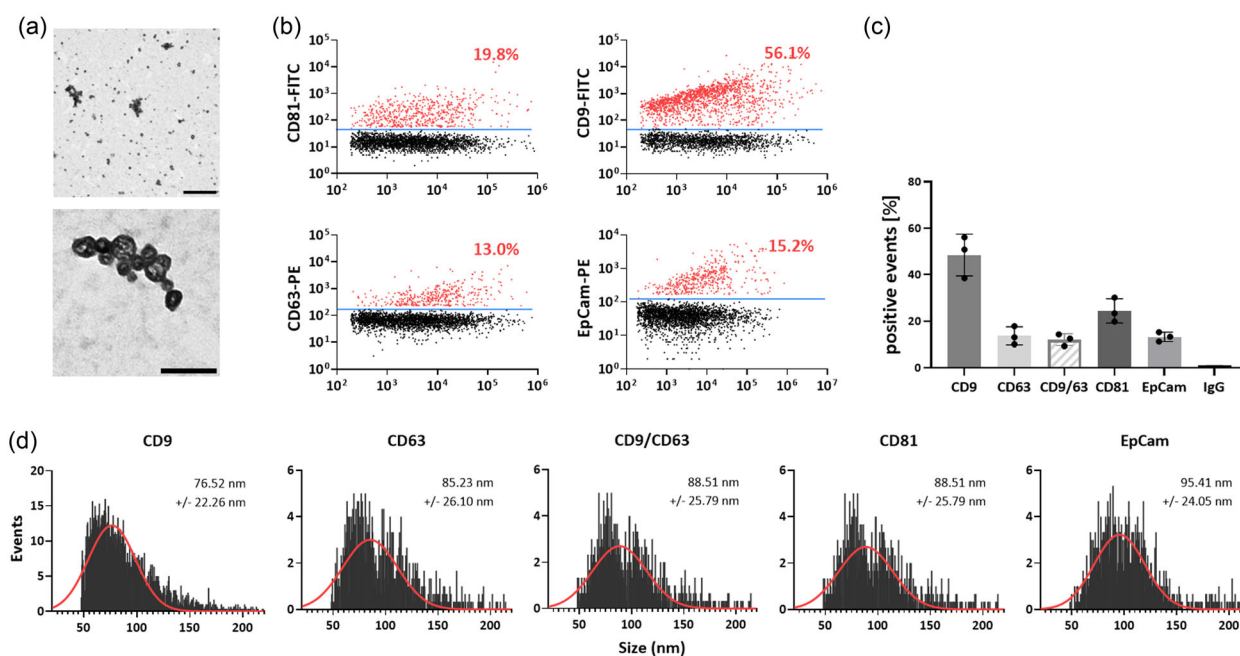


FIGURE 5 FFE allows purification of bona fide EVs from ascites. (a) Electron microscopy of purified vesicles. EVs were counterstained by uranyl acetate and are shown in two different magnifications. Scale bar, 500 nm (top); 100 nm (bottom). (b) Single-particle phenotyping of ascites-derived EVs. FITC-coupled anti-CD9 and anti-CD81 and PE-coupled anti-CD63 and anti-EpCAM antibodies at 12.5 nM were incubated with particles in a final volume of 50 μ l freshly filtered PBS (0.1 μ m ϕ). After staining, all samples were washed, ultracentrifuged, and suspended in the same volume (50 μ l) of freshly filtered PBS (0.1 μ m ϕ) before fluorescence measurement by nFCM. (c) Individual examples of phenotypic characterization of EVs from panel c. Bivariate dot plots of the indicated fluorescence against SSC are shown. (d) Nanoflow cytometry analysis, depicting the size distribution (diameter) of particles positive for the indicated markers and indicating the mean of the size distribution calculated by gaussian fit

challenging. In particular, various body fluids such as blood (plasma and serum), urine, milk, and ascites expose highly heterogeneous EV subpopulations, which may overlap in size, density, and marker proteins, representing a significant challenge in the purification process (Brennan et al., 2020; Mateescu et al., 2017). In addition, to achieve the required purity, most methods are based on very laborious and time-consuming processes, hampering throughput.

Here we demonstrate a time-efficient purification of EVs from primary heterogeneous and protein-rich starting material (ascites) using FFE and characterize their physical and biological properties with state-of-the-art technologies. Furthermore, high reproducibility of the methodology was achieved, which cannot always be secured by other methods, especially for primary biomaterials or patient samples. Since FFE is highly adaptable to different particle populations due to its underlying technological principle, protocols can easily be adapted to the needs of the respective applications. This applies to different biofluids, as they may differ in terms of the amount of protein and consequently in their conductivity. For example, urine has a relatively low conductivity compared to blood samples due to its low protein content. However, by using the FFE protocol established

here, preliminary data show that different biofluids vary only slightly in terms of their separation (data not shown). Thus, a mid-throughput sample throughput can be achieved, separating 100 samples every 6 h, principally qualifying FFE for use in a clinical setting for the separation of EVs and detection of EV-associated biomarkers. In general, a relatively broad range of input volumes can be processed by FFE, although sample sizes from 500 μ l to 4 ml have been found to be the most feasible in our experiments. Technically, however, it is also possible to concentrate larger volumes, such as urine, prior FFE by ultra-filtration or comparable methods. Here, the conductivity of the respective media should always be taken into account.

In addition, FFE avoids the harsh mechanical forces that occur during ultracentrifugation and can affect the integrity of EVs, thus loosely associated factors are dislodged from the EV corona, resulting in the loss of functionally important properties (Mol et al., 2017; Wolf et al., 2022). However, one cannot exclude the subtraction of loosely associated factors from the so-called soft corona by the electrostatic forces during electrophoresis. Nonetheless, the FFE represents a low-impact separation approach in which resolution depends on the selected pH of the buffers and allows isolation of the most native EV possible as confirmed by our initial functional analyses. However, further in-depth studies are needed to evaluate the enrichment of potential native EVs using FFE.

However, it should be considered that the primary material used here has to be diluted at least 1:2, since ascites, like any comparable primary material (such as blood plasma), is relatively protein-rich. This is connected with a relatively high molar conductivity of the respective inputs, which can significantly impair separation performance during electrophoresis. Furthermore, FFE necessitates extensive technical expertise and specific equipment, thus limiting its universal applicability.

Given the flexibility and tuneability of FFE, it might be feasible to separate distinct EV subpopulations through their zeta potential and thus gain more precise insight into the composition of the total particle population. A directly applicable prominent additional advantage beyond the specific fractionation of EVs is, that secreted soluble components may be separated and collected according to their charge in parallel and thus subsequently analyzed in full secretome approaches.

As common with many other approaches, FFE is not necessarily a stand-alone EV-separation method. In particular, final ultrafiltration might be needed as described in this article to reduce the sample volume and increase the particle concentration. Here, 96-well formats could also be adopted to ensure a high sample throughput.

Although a mid-throughput approach is feasible with this, a transfer of the technology into clinical applications may require further developments. To that end, simplification through a reduced number of buffers used, a more compact design, and protocol improvements, such as the addition of non-ionic surfactants to enhance the running behaviour of EVs, come immediately to mind as avenues to pursue.

In sum, FFE is a novel method that is applicable for the purification of EVs as well as other components of the full secretome from highly complex samples with high throughput making it appropriate not only for small-scale laboratory analysis but also offering the potential for future clinical applications.

AUTHOR CONTRIBUTIONS

Christian Preußer and Elke Pogge von Strandmann designed the study, interpreted the data, and wrote the article. Christian Preußer, Kathrin Stelter, Gerhard Weber, Tobias Tertel, Witold Szymanski and Manuel Linder performed experiments. Frederik Helmprobst performed electron microscopy experiments. Gerhard Weber, Bernd Giebel, Johannes Graumann, Silke Reinartz, Rolf Müller edited this manuscript. All authors read and corrected the article.

ACKNOWLEDGEMENTS

We thank Bettina Lehman for providing blood plasma and serum samples. We thank Kenneth W. Witwer and members of our group for discussions and comments on the manuscript. Part of this work was supported by the Deutsche Forschungsgemeinschaft (GRK 2573/1 project 416910386, to E. PvS.).

CONFLICTS OF INTEREST

GW is CEO and founder of FFE Service GmbH. Other authors declare that there are no conflicts of interest. GW filed a patent application on the use of FFE for isolating extracellular vesicles (EP 20213560.4, 'Free Flow Electrophoresis Method for separating analytes'; patent pending)

ORCID

Christian Preußer  <https://orcid.org/0000-0002-5183-4262>

Johannes Graumann  <https://orcid.org/0000-0002-3015-5850>

Elke Pogge von Strandmann  <https://orcid.org/0000-0003-4785-9165>

REFERENCES

Akagi, T., & Ichiki, T. (2008). Cell electrophoresis on a chip: What can we know from the changes in electrophoretic mobility? *Analytical and Bioanalytical Chemistry*, 391, 2433–2441.

- Brennan, K., Martin, K., Fitzgerald, S. P., O'Connell, J., Wu, Y., Blanco, A., Richardson, C., & Mc Gee, M. M. (2020). A comparison of methods for the isolation and separation of extracellular vesicles from protein and lipid particles in human serum. *Scientific Reports*, *10*, 1039. <https://doi.org/10.1038/s41598-020-57497-7>
- Clayton, A., Boilard, E., Buzas, E. I., Cheng, L., Falcón-Perez, J. M., Gardiner, C., Gustafson, D., Gualerzi, A., Hendrix, A. N., Hoffman, A., Jones, J., Lässer, C., Lawson, C., Lenassi, M., Nazarenko, I., O'Driscoll, L., Pink, R., Siljander, P. R. M., Soekmadji, C., ... Nieuwland, R. (2019). Considerations towards a roadmap for collection, handling, and storage of blood extracellular vesicles. *Journal of Extracellular Vesicles*, *8*, 1647027.
- Dörsam, B., Bösl, T., Reiners, K. S., Barnert, S., Schubert, R., Shatnyeva, O., Zigrino, P., Engert, A., Hansen, H. P., & Von Strandmann, E. P. (2018). Hodgkin lymphoma-derived extracellular vesicles change the secretome of fibroblasts toward a CAF phenotype. *Frontiers in Immunology*, *9*, 1358.
- Dörsam, B., Reiners, K. S., & Von Strandmann, E. P. (2018). Cancer-derived extracellular vesicles: Friend and foe of tumour immunosurveillance. *Philosophical Transactions of the Royal Society B: Biological Sciences*, *373*, 20160481.
- Karimi, N., Cvjetkovic, A., Jang, S. C., Crescitelli, R., Hosseinpour Feizi, M. A., Nieuwland, R., LÄ Tvall, J., & LÄ Sser, C. (2018). Detailed analysis of the plasma extracellular vesicle proteome after separation from lipoproteins. *Cellular and Molecular Life Sciences*, *75*(15), 2873–2886.
- Krivánková, L., & Bocek, P. (1998). Continuous free-flow electrophoresis. *Electrophoresis*, *19*, 1064–1074.
- Linares, R., Tan, S., Gounou, C., Arraud, N., & Brisson, A. R. (2015). High-speed centrifugation induces aggregation of extracellular vesicles. *Journal of Extracellular Vesicles*, *4*, 29509.
- Mateescu, B., Kowal, E. J. K., Van Balkom, B. W. M., Bartel, S., Bhattacharyya, S. N., Buzás, E. I., Buck, A. H., De Candia, P., Chow, F. W. N., Das, S., Driedonks, T. A. P., Fernández-Messina, L., Haderk, F., Hill, A. F., Jones, J. C., Van Keuren-Jensen, K. R., Lai, C. P., Lässer, C., Di Liegro, I., ... Nolte-Hoen, E. N. M. (2017). Obstacles and opportunities in the functional analysis of extracellular vesicle RNA—An ISEV position paper. *Journal of Extracellular Vesicles*, *6*, 1286095.
- Mol, E. A., Goumans, M.-J., Doevendans, P. A., Sluijter, J. P. G., & Vader, P. (2017). Higher functionality of extracellular vesicles isolated using size-exclusion chromatography compared to ultracentrifugation. *Nanomedicine*, *13*, 2061–2065.
- Staubach, S., Tertel, T., Walkenfort, B., Buschmann, D., & Pfaffl, M. W. (2022). *Free flow electrophoresis allows quick and reproducible preparation of extracellular vesicles from conditioned cell culture media*. *Extracell Vesicles Circ Nucleic Acids*.
- Théry, C., Amigorena, S., Raposo, G., & Clayton, A. (2006). Isolation and characterization of exosomes from cell culture supernatants and biological fluids. *Current Protocols in Cell Biology*, Chapter 3, Unit 3.22.
- Théry, C., Witwer, K. W., Aikawa, E., Alcaraz, M. J., Anderson, J. D., Andriantsitohaina, R., Antoniou, A., Arab, T., Archer, F., Atkin-Smith, G. K., Ayre, D. C., Bach, J.-M., Bachurski, D., Baharvand, H., Balaj, L., Baldacchino, S., Bauer, N. N., Baxter, A. A., Bebawy, M., ... Zuba Surma, E. K. (2018). Minimal information for studies of extracellular vesicles 2018 (MISEV2018): A position statement of the International Society for Extracellular Vesicles and update of the MISEV2014 guidelines. *Journal of Extracellular Vesicles*, *7*, 1535750.
- Tertel, T., Bremer, M., Maire, C., Lamszus, K., Peine, S., Jawad, R., Andaloussi, S. E. L., Giebel, B., Ricklefs, F. L., & Görgens, A. (2020a). High-resolution imaging flow cytometry reveals impact of incubation temperature on labeling of extracellular vesicles with antibodies. *Cytometry A*, *97*, 602–609.
- Tertel, T., Görgens, A., & Giebel, B. (2020b). Analysis of individual extracellular vesicles by imaging flow cytometry. *Methods Enzymol*, *645*, 55–78.
- Tertel, T., Tomić, S., Đokić, J., Radojević, D., Stevanović, D., Ilić, N. A., Giebel, B., & Kosanović, M. (2022). Serum-derived extracellular vesicles: Novel biomarkers reflecting the disease severity of COVID-19 patients. *Journal of Extracellular Vesicles*, *11*, e12257.
- Tulkens, J., De Wever, O., & Hendrix, A. n (2020). Analyzing bacterial extracellular vesicles in human body fluids by orthogonal biophysical separation and biochemical characterization. *Nature Protocols*, *15*(1), 40–67.
- Van Der Pol, E., Coumans, F. A. W., Grootemaat, A. E., Gardiner, C., Sargent, I. L., Harrison, P., Sturk, A., Van Leeuwen, T. G., & Nieuwland, R. (2014). Particle size distribution of exosomes and microvesicles determined by transmission electron microscopy, flow cytometry, nanoparticle tracking analysis, and resistive pulse sensing. *Journal of Thrombosis and Haemostasis*, *12*(7), 1182–1192. <https://doi.org/10.1111/jth.12602>
- Van Niel, G., Bergam, P., Di Cicco, A., Hurbain, I., Lo Cicero, A., Dingli, F., Palmulli, R., Fort, C., Potier, M. C., Schurgers, L. J., Loew, D., Levy, D., & Raposo, G. (2015). Apolipoprotein E regulates amyloid formation within endosomes of pigment cells. *Cell Reports*, *13*, 43–51.
- Van Niel, G., D'angelo, G., & Raposo, G. (2018). Shedding light on the cell biology of extracellular vesicles. *Nature Reviews Molecular Cell Biology*, *19*, 213–228.
- Weber, P. J. A., Weber, G., & Eckerskorn, C. (2004). Isolation of organelles and prefractionation of protein extracts using free-flow electrophoresis. *Current Protocols in Protein Science*, Chapter 22, Unit 22.5.
- Welsh, J. A., Van Der Pol, E., Arkesteijn, G. J. A., Bremer, M., Brisson, A., Coumans, F., Dignat-George, F., Duggan, E., Ghiran, I., Giebel, B., Görgens, A., Hendrix, A., Lacroix, R., Lannigan, J., Libregts, S. F. W. M., Lozano-Andrés, E., Morales Kastresana, A., Robert, S., De Rond, L., ... Jones, J. C. (2020). MIFlowCyt-EV: A framework for standardized reporting of extracellular vesicle flow cytometry experiments. *Journal of Extracellular Vesicles*, *9*, 1713526.
- Witwer, K. W., & Théry, C. (2019). Extracellular vesicles or exosomes? On primacy, precision, and popularity influencing a choice of nomenclature. *Journal of Extracellular Vesicles*, *8*, 1648167.
- Wolf, M., Poupardin, R. W., Ebner-Peking, P., Andrade, A. C., Blöchl, C., Obermayer, A., Gomes, F. G., Vari, B., Maeding, N., Eminger, E., Binder, H. M., Raninger, A. M., Hochmann, S., Bracht, G., Spittler, A., Heuser, T., Ofir, R., Huber, C. G., Aberman, Z., ... Strunk, D. (2022). A functional corona around extracellular vesicles enhances angiogenesis, skin regeneration and immunomodulation. *Journal of Extracellular Vesicles*, *11*, e12207.
- Zhang, H., & Lyden, D. (2019). Asymmetric-flow field-flow fractionation technology for exomere and small extracellular vesicle separation and characterization. *Nature Protocols*, *14*, 1027–1053.

SUPPORTING INFORMATION

Additional supporting information can be found online in the Supporting Information section at the end of this article.

How to cite this article: Preußner, C., Stelter, K., Tertel, T., Linder, M., Helmprobst, F., Szymanski, W., Graumann, J., Giebel, B., Reinartz, S., Müller, R., Weber, G., & von Strandmann, E. P. (2022). Isolation of native EVs from primary biofluids—Free-flow electrophoresis as a novel approach to purify ascites-derived EVs. *Journal of Extracellular Biology*, *1*, e71. <https://doi.org/10.1002/jex2.71>